Atmos. Meas. Tech., 10, 989–997, 2017
www.atmos-meas-tech.net/10/989/2017/
doi:10.5194/amt-10-989-2017

Atmospheric Measurement Techniques
Open Access

Technical note: Sensitivity of instrumental line shape monitoring for the ground-based high-resolution FTIR spectrometer with respect to different optical attenuators

Youwen Sun[1,2,*], **Mathias Palm**[3,*], **Christine Weinzierl**[3], **Christof Petri**[3], **Justus Notholt**[3], **Yuting Wang**[3], and **Cheng Liu**[4,2,1]

[1]Key Laboratory of Environmental Optics and Technology, Anhui Institute of Optics and Fine Mechanics, Chinese Academy of Sciences, 230031 Hefei, China
[2]Center for Excellence in Urban Atmospheric Environment, Institute of Urban Environment, Chinese Academy of Sciences, 361021 Xiamen, China
[3]University of Bremen, Institute of Environmental Physics, P.O. Box 330440, 28334 Bremen, Germany
[4]University of Science and Technology of China, Hefei, 230026, China
[*]These authors contributed equally to this work.

Correspondence to: Cheng Liu (chliu81@ustc.edu.cn)

Received: 6 January 2016 – Discussion started: 8 March 2016
Revised: 17 September 2016 – Accepted: 11 October 2016 – Published: 13 March 2017

Abstract. The TCCON (Total Carbon Column Observing Network) and most NDACC (Network for Detection of Atmospheric Composition Change) sites assume an ideal ILS (instrumental line shape) for analysis of the spectra. In order to adapt the radiant energy received by the detector, an attenuator or different sizes of field stop can be inserted in the light path. These processes may alter the alignment of a high-resolution FTIR (Fourier transform infrared) spectrometer, and may result in bias due to ILS drift. In this paper, we first investigated the sensitivity of the ILS monitoring with respect to application of different kinds of attenuators for ground-based high-resolution FTIR spectrometers within the TCCON and NDACC networks. Both lamp and sun cell measurements were conducted after the insertion of five different attenuators in front of and behind the interferometer. The ILS characteristics derived from lamp and sun spectra are in good agreement. ILSs deduced from all lamp cell measurements were compared. As a result, the disturbances to the ILS of a high-resolution FTIR spectrometer with respect to the insertion of different attenuators at different positions were quantified. A potential strategy to adapt the incident intensity of a detector was finally deduced.

1 Introduction

In order to achieve consistent results between different FTIR (Fourier transform infrared) sites, the TCCON (Total Carbon Column Observing Network, http://www.tccon.caltech.edu/) and NDACC (Network for Detection of Atmospheric Composition Change; http://www.ndacc.org/) have developed strict data acquisition and retrieval methods for minimizing the site to site differences (Kurylo, 1991; Davis et al., 2001; Washenfelder, 2006; Schneider et al., 2008; Hannigan and Coffey, 2009; Messerschmidt et al., 2010; Wunch et al., 2010, 2011; Kohlhepp et al., 2011; Hase et al., 2012; Wang et al., 2016). Interferograms are acquired with similar instruments operated with common detectors, acquisition electronics, and/or optical filters. These interferograms are first converted to spectra and later to retrieved products using dedicated processing algorithms, i.e., GFIT, PROFFIT, or SFIT (Hase et al., 2006; Hannigan and Coffey, 2009; Wunch et al., 2010, 2015). However, biases between sites may arise due to the behavior of individual spectrometers, if not properly characterized. Some of these differences result from a misalignment of an interferometer, which can change abruptly as a consequence of operator intervention or drift slowly due to mechanical degradation over time (Olsen et al., 2004; Miller et al., 2007; Duchatelet et al., 2010; Hase et al., 2013; Feist et al., 2016). These misalignment effects can be diagnosed via the monitoring of instrumental line shape (ILS) (Hase et al., 1999, 2013). It has become a part of FTIR network practice to regularly use a low-pressure calibration gas cell (HBr or HCl) to diagnose a misalignment of the spectrometer and to realign the instrument when indicated (Hase et al., 1999, 2013; Wunch et al., 2010, 2015). A successful alignment scheme for high-resolution spectrometers was proposed about a decade ago and has become the standard alignment procedure for both TCCON and NDACC (Hase et al., 2013). As a result, the individual systematic errors and site to site biases caused by misalignment due to mechanical degradation are already minimized. However, the ILS measurements are commonly performed using an internal lamp. For the gas measurements, the ILS of the whole system (i.e., including the solar tracking system and the entrance optics) is also of utmost importance (F. Hase and T. Blumenstock, personal communication, 2011).

The TCCON and many NDACC assume an ideal ILS in spectra retrieval. In the TCCON network a maximal variation of the ILS is prescribed, on which the maximal variation for modulation efficiency (ME) amplitude is 5 % (Wunch et al., 2011, 2015). This assumption still holds within the required accuracy of the results. The TCCON prescribes a constant entrance field stop. In order to adapt the intensity of the incident radiation, an attenuator is inserted in the light path. The NDACC changes the entrance field stop size if incident radiation changes. These processes may alter the alignment of a high-resolution FTIR spectrometer and subsequently result in biases due to ILS drift. An alternative way that does not alter the alignment of a spectrometer is done via the selection of a suitable amplifier gain, depending on incoming intensities. However, this method has limited contribution and may be plagued with deteriorating SNR (signal-to-noise ratio) of the spectrum. For measurement performed within the TCCON and NDACC networks, the degree of ILS changes caused by the above processes is not fully quantified. In this paper, we designed experiments to investigate the sensitivity of ILS monitoring for ground-based high-resolution FTIR spectrometers with respect to different optical attenuators.

2 Experimental design

2.1 Experiment description

All experiments were performed with a Bruker FTS (Fourier transform spectrometer) 125HR located in Bremen, Germany. This instrument is operated by the Institute of Environmental Physics (IUP), University of Bremen, Germany, and it has been part of the networks NDACC and TCCON since 2004 (Messerschmidt et al., 2010). The instrument's alignment is regularly checked using a gas cell filled with a known amount of either HBr or HCl. NDACC ILS monitoring uses a cell 2 cm long filled with 2 mbar of HBr. TCCON ILS monitoring uses a cell 10 cm long filled with 5 mbar of HCl. The optical scenarios for routine check are listed in Table 1. In this study, these optical scenarios are called default scenarios.

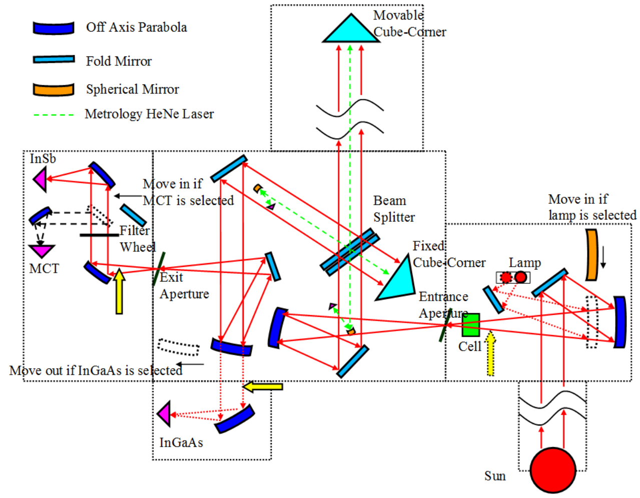

Figure 1. Schematic drawing of the instrument with all its mirrors. The yellow arrows show the place where the attenuators are inserted. The solid yellow arrows are for the group one experiments; i.e., the attenuator was inserted to a specified place just in front of the exit parabolic mirror. The dotted yellow arrow is for the group two experiments; i.e., the attenuator was inserted to a specified place between the entrance parabolic/spherical mirror and its focus (i.e., the position of the 1 mm entrance field stop).

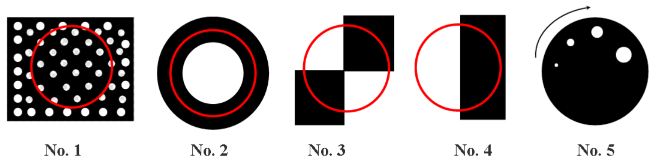

Figure 2. Five different attenuators used in the experiment. The red circle indicates the size of the beam. Check the text for detailed descriptions.

The LINEFIT software is used for the ILS calculations (Hase et al., 1999). It retrieves a complex ME as a function of optical path difference (OPD), which is represented by a ME amplitude, the real part of the complex ME, and a ME phase error, its imaginary part (Hase et al., 1999). The ME amplitude refers to the width of the ILS, while the ME phase error quantifies the degree of ILS asymmetry (Hase et al., 2013). LINEFIT offers two fitting modes. The micro window (WM) mode fits each absorption line separately, and the broadband mode fits all absorption lines simultaneously. For comparison, the WM mode rather than broadband mode was used for all ILSs' retrieval, and all spectra were normalized to the same level before analysis.

Five different kinds of attenuators (Fig. 2) were used in the experiments. Attenuator no. 1 is a flat metal perforated

Table 1. Optical scenarios for each ILS monitoring.

Items		Scenarios							
		Light source	Cell	Entrance field stop	Attenuator type	Attenuator position	Beam splitter	Detector	Filter
Routine check	TCCON	tungsten	HCl		none	–	CaF_2	InGaAs	none
	NDACC	globar	HBr				KBr	InSb	OF3[b]
Group one (G1)	TCCON	tungsten or sun	HCl	1 mm	no. 1–4	detector compartment	CaF_2	InGaAs	none
	NDACC	globar or sun	HBr				KBr	InSb	OF3
Group two (G2)	TCCON	tungsten or sun	HCl			source compartment	CaF_2	InGaAs	none
	NDACC	globar or sun	HBr				KBr	InSb	OF3
Group three (G3)	TCCON	tungsten or sun	HCl	no. 5 (0.8 or 1.2 mm)[a]		entrance aperture	CaF_2	InGaAs	none
	NDACC	globar or sun	HBr				KBr	InSb	OF3

[a] Attenuator no. 5 is an entrance field stop other than 1 mm size. [b] CWN (center wave number) = 2300 cm^{-1}, and FWHM (full width at half maximum) = 500 cm^{-1}.

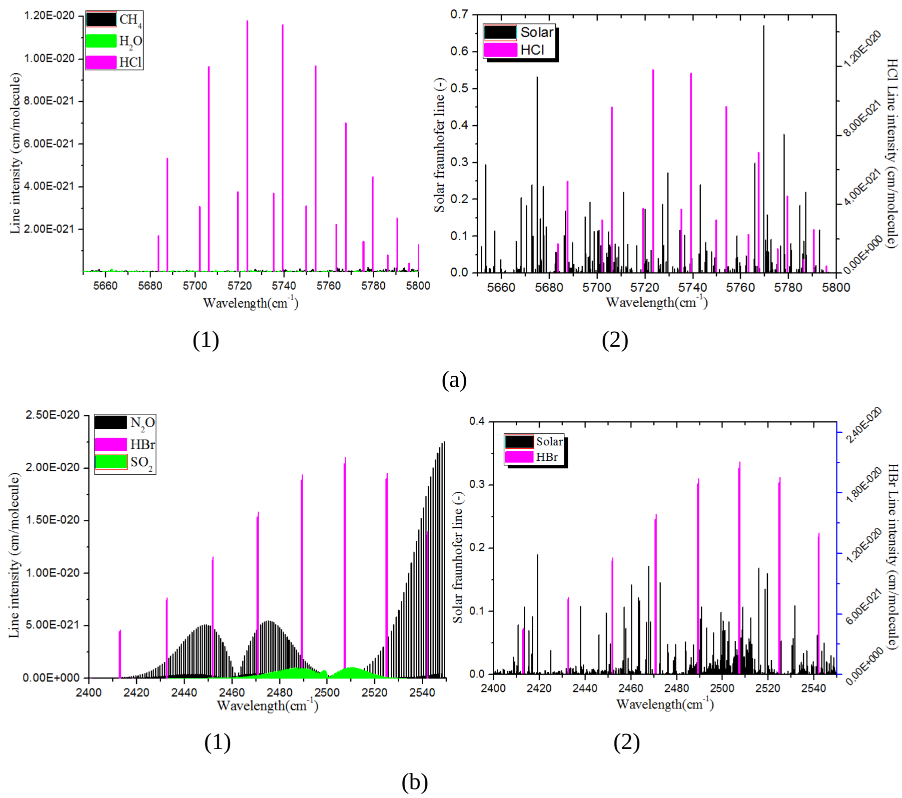

Figure 3. Typical interfering gases and the solar Fraunhofer lines within the HCl and HBr fitting regions. Panel **(a1)** shows the interfering gases within the HCl fitting regions, **(a2)** shows the solar Fraunhofer lines within the HCl fitting regions, **(b1)** shows the interfering gases within the HBr fitting regions, and **(b2)** shows the solar Fraunhofer lines within the HBr fitting regions. The absorption intensities of all gases are adopted from HITRAN2008. The solar Fraunhofer lines are adopted from the input files of the TCCON software GGG2014.

on a regular grid. Attenuator no. 2 restricts the diameter of a beam. Attenuator no. 3 blocks the opposite 1/4 pairs of a beam and lets the rest 1/4 pairs pass through. Attenuator no. 4 blocks half of a beam. Attenuator no. 5 is an entrance field stop other than the 1 mm size, i.e., a 0.8 or 1.2 mm field stop located in the entrance aperture wheel. It has to be noted that theoretically, all field stops are equivalent; however, in practice they are not because the real instruments are not as symmetric as required by theory. The reproducibility of me-

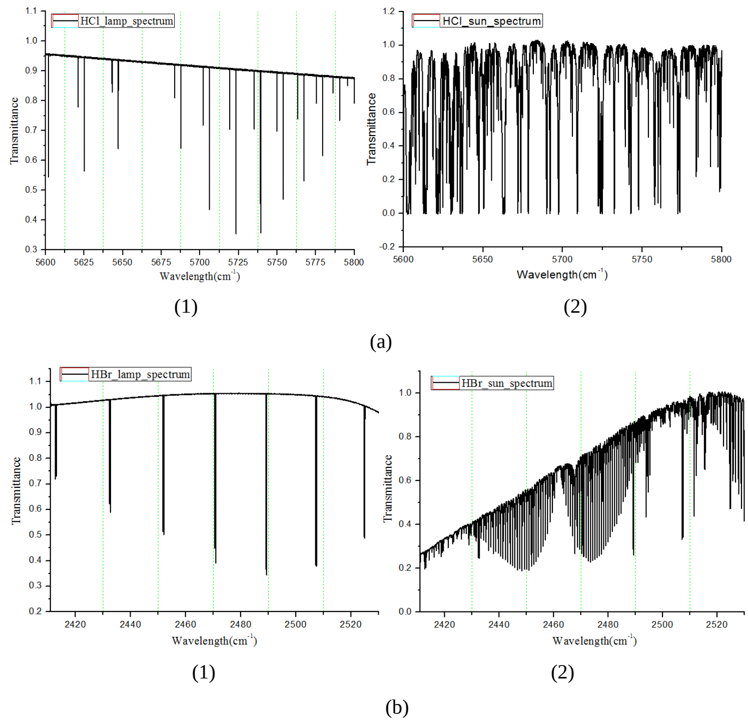

Figure 4. Normalized spectra used for ILS retrievals. Panel **(a1)** is a lamp spectrum for the TCCON HCl cell measurement, **(a2)** is a solar spectrum for the TCCON HCl cell measurement, **(b1)** is a lamp spectrum for the NDACC HBr cell measurement, and **(b2)** is a solar spectrum for the NDACC HBr cell measurement. Less interfering structures in lamp spectra than solar spectra are shown.

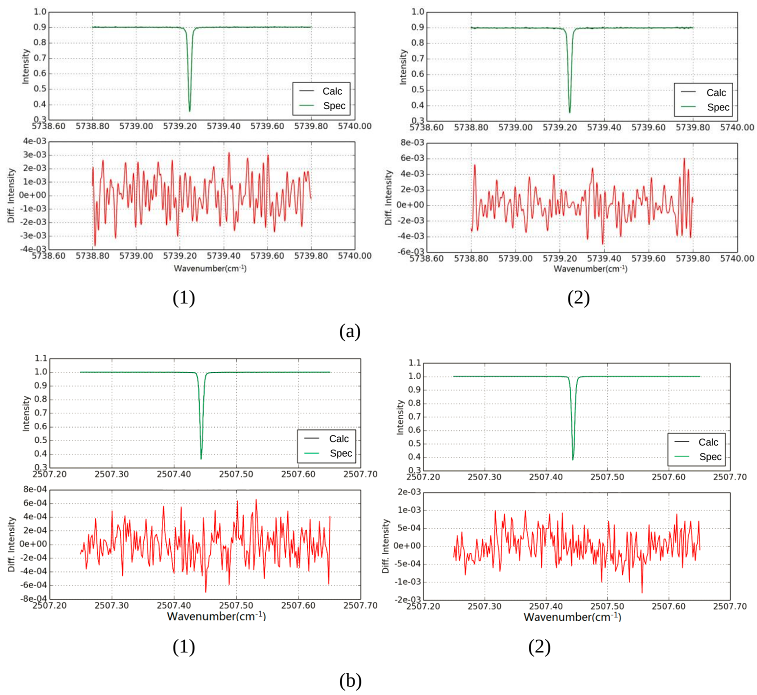

Figure 5. The LINEFIT-fitted cases for TCCON and NDACC after background removal. Panel **(a1)** is the TCCON ILS fitting using a lamp spectrum, **(a2)** is the TCCON ILS fitting using a solar spectrum, **(b1)** is the NDACC ILS fitting using a lamp spectrum, and **(b2)** is the NDACC ILS fitting using a solar spectrum. Only one micro window for each case is shown, and the residual in most cases is less than 0.2 %. "calc" represents the calculated spectrum, and "spec" represents the measured spectrum.

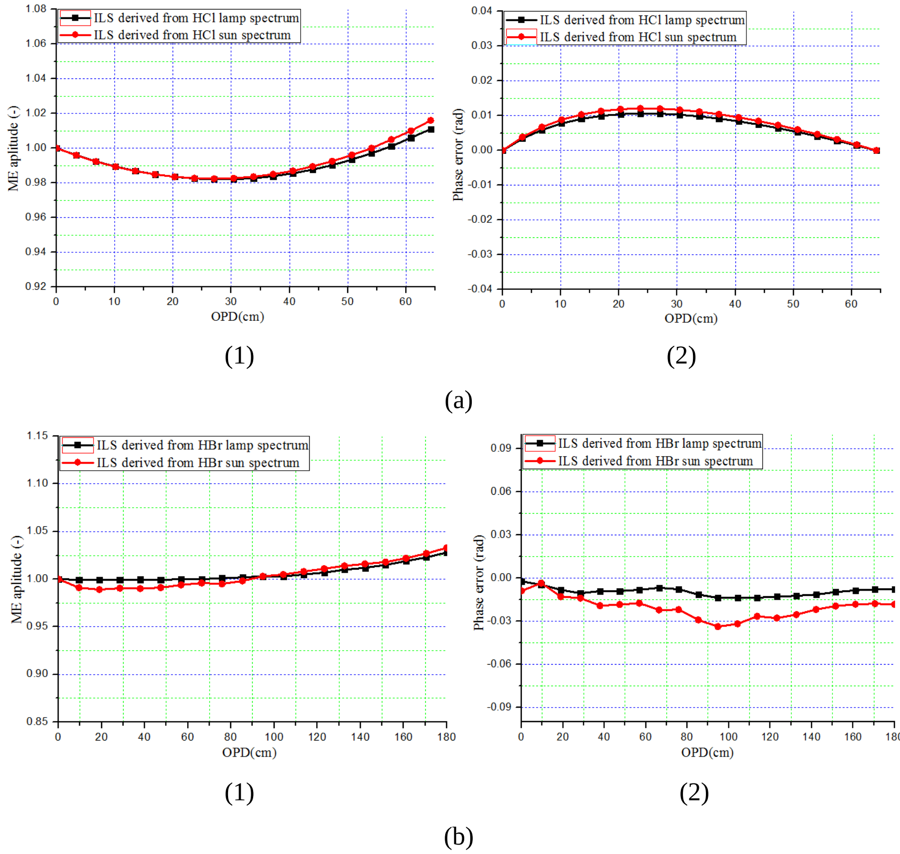

Figure 6. ILS retrievals derived from lamp (black lines) and sun spectra (red lines). Panel **(a1)** shows ILS modulation efficiencies deduced from HCl lamp and sun spectra, **(a2)** shows ILS phase errors deduced from HCl lamp and sun spectra, **(b1)** shows ILS modulation efficiencies deduced from HBr lamp and sun spectra, and **(b2)** shows ILS phase errors deduced from HBr lamp and sun spectra.

chanical setups, like the position of the entrance aperture, is also not always granted to a high degree.

We performed three groups of experiments within 3 weeks. The alignment during these experiments was not changed and was constant. This is backed up by experience, i.e., the past monitoring of the ILS at the instruments operated by the Universität Bremen, which showed that the ILS only changes very slowly if ambient conditions are stable. Each TCCON lamp and sun cell measurement was repeated 60 and 6 times, and for NDACC, 50 and 4 times, respectively. Fewer repetitions were done for the solar measurements to minimize the effect of atmospheric variations.

2.2 Group one experiment (G1)

One of the attenuators no. 1–4 is inserted at a specified place just in front of the exit parabolic mirror (Fig. 1). It was made up of four sun cell measurements and four lamp cell measurements. All sun cell measurements were performed within 1 day with a clear sky condition suitable for observations. The optical scenarios for group one measurement are listed in Table 1. The attenuators for the TCCON and NDACC are in the parallel beam and in the divergent beam, respectively.

2.3 Group two experiment (G2)

As shown in Fig. 1 and Table 1, G2 is the same as G1 except that one of the attenuators no. 1–4 was inserted at a specified place between the entrance parabolic/spherical mirror and its focus (i.e., the position of the 1 mm entrance field stop). For both TCCON and NDACC, the attenuators are in the divergent beam.

2.4 Group three experiment (G3)

As shown in Table 1, none of the attenuators no. 1–4 was inserted into the light path, but an entrance field stop other than the default 1 mm size was selected. In this manner, the attenuator no. 5 is in the image of the light source for both TCCON and NDACC.

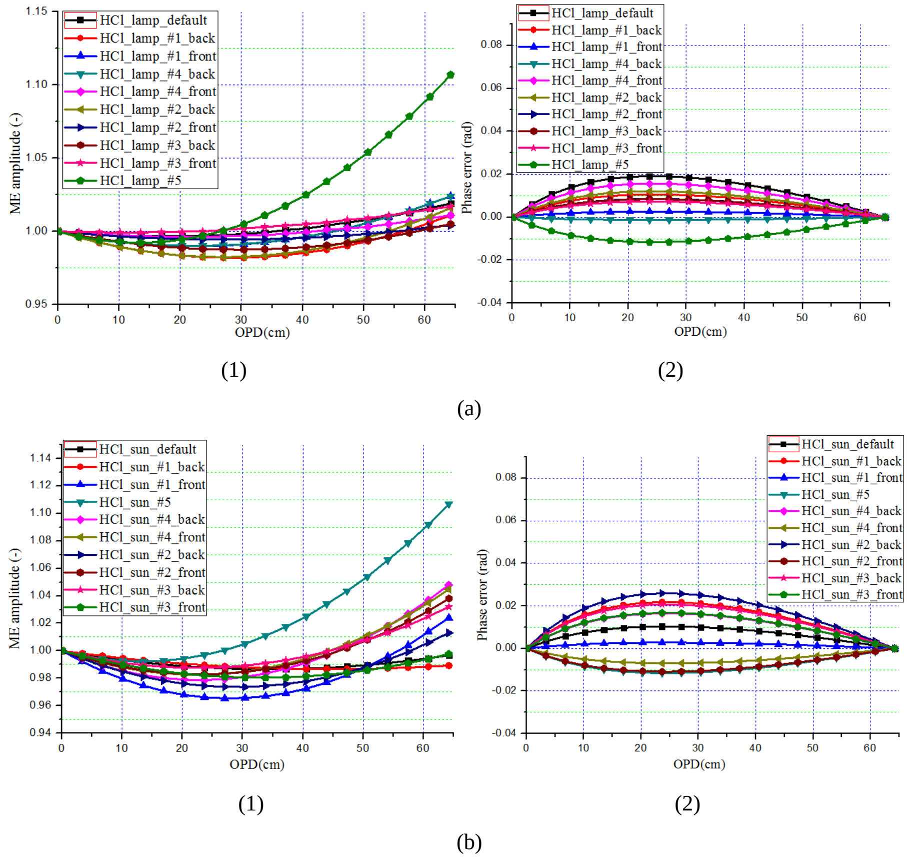

Figure 7. TCCON ILS retrievals for different attenuators. Panels **(a)** and **(b)** are ILS retrievals derived from lamp and sun cell measurements, respectively. (1) and (2) of each subplot represent the ME amplitude and phase error, respectively. "HCl_sun_#3_front" represents the sun HCl cell measurement performed by inserting the attenuator no. 3 in front of the interferometer. The nomenclature for other plot labels is straightforward.

3 Consistency between sun and lamp ILSs

In Fig. 3, the typical interfering gases and the solar Fraunhofer lines within the HCl and HBr fitting regions are shown. In the TCCON case, H_2O and CH_4 have non-negligible absorptions in the same region as HCl. The NDACC case is more complicated; both N_2O and SO_2 show strong interferences in HBr region. Furthermore, non-negligible solar Fraunhofer lines within both HCl and HBr regions are shown. Therefore, optical background removal is rather important, especially for the sun cell measurement. Since the interfering items in the solar spectrum are not easy to quantify, each target spectrum (with a cell inserted in the optical path) is divided by a reference spectrum (without a cell inserted into the optical path) to remove the optical background.

The default scenarios were used to examine the consistency between the lamp and sun ILS retrieval. Typical lamp and sun spectra used for TCCON and NDACC ILS retrievals are shown in Fig. 4. The sun spectra in both HCl and HBr regions exhibited more interference than the lamp spectra. The lamp spectra are nearly free of interference except the non-constant transmission due to the glass body of the gas cells, whereas the atmospheric structures are obviously shown in sun spectra.

Figure 5 shows the fitted cases for TCCON and NDACC ILS retrievals after removing the optical background. LINEFIT achieved good ILS fittings for both TCCON and NDACC regardless of lamp or sun spectrum. The ILS modulation efficiencies and phase errors deduced from Fig. 5 are shown in Fig. 6. It concludes that the lamp and solar spectrum can achieve consistent ILS retrievals for both TCCON and NDACC, though the solar spectrum is much more structured than the lamp spectrum. The three groups of experiments deduced the same conclusion.

4 Sensitivity study

4.1 ILS retrieval sensitivity

The TCCON and NDACC ILS retrievals derived from each group experiment are presented in Figs. 7 and 8, respectively. The variation of the ILSs retrieved from lamp cell measure-

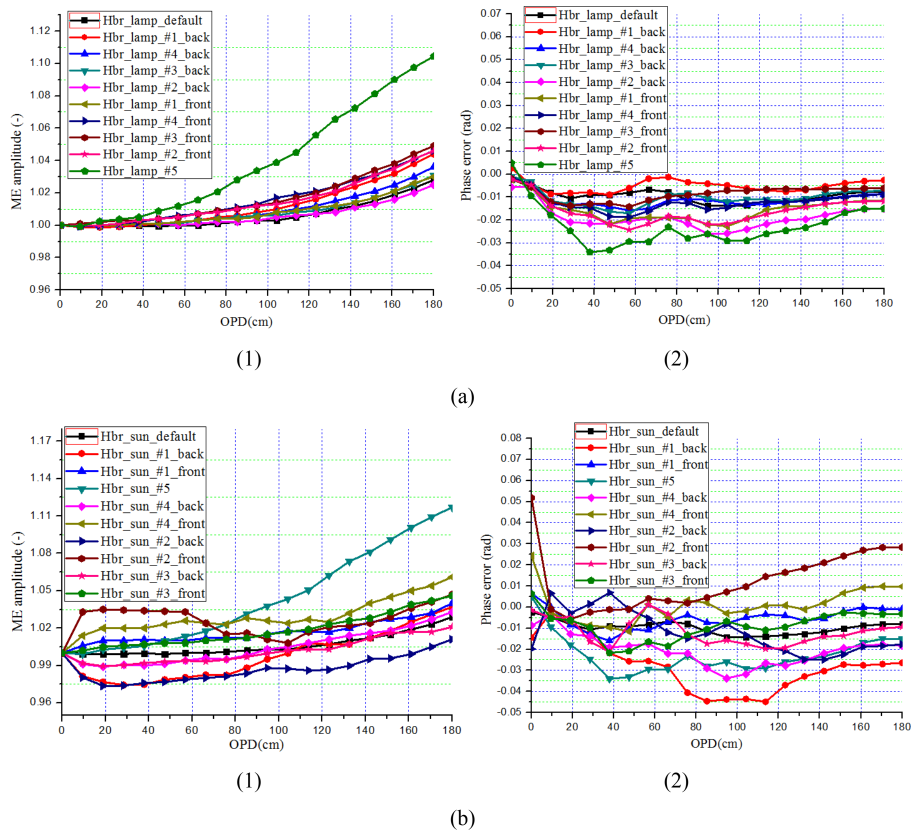

Figure 8. The same as Fig. 7 but for NDACC.

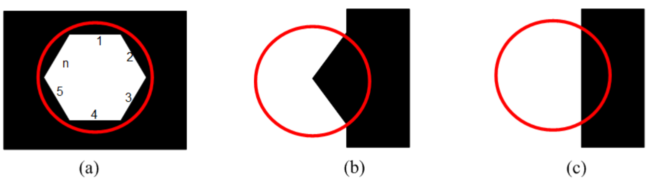

Figure 9. Typical derivatives of attenuators no. 1–4 as potentials to decrease the incident intensity. Panel **(a)** is a derivative of attenuator no. 2, which restricts the diameter of a beam with a polygon. Panel **(b)** is derivative of attenuator no. 3, which blocks a beam with an arc of sector. Panel **(c)** is a derivative of attenuator no. 4, which partly blocks a beam.

ments are smaller than those retrieved from sun cell measurements for two reasons: first, we performed more repeat measurements for each lamp cell measurement than for sun cell measurement; therefore the random noise is lower. In addition, the simpler measurement scenario makes the optical background removal of the lamp cell measurement easier and better.

The ILS variation caused by inserting attenuators no. 1–4 is much less than attenuator no. 5. Both TCCON and NDACC ILSs derived from inserting attenuators no. 1–4 are close to the ILS derived from the default optical scenario, with a ME amplitude change of $< 3\,\%$ within $\mathrm{OPD_{max}} = 45$ cm and $< 6\,\%$ within $\mathrm{OPD_{max}} = 180$ cm, respectively. Both TCCON and NDACC ILSs derived from attenuators no. 5 are larger than 8 % at the $\mathrm{OPD_{max}}$. This is most likely because the routine alignment adjustment was performed by using a specified 1 mm entrance field stop, and the consistency between different field stops produces a non-negligible optical misalignment if a field stop other than the 1 mm size was selected. Note that the different aperture size was taken into account in the ILS determination. This is most likely because of mechanical inaccuracies in the mechanics of the entrance aperture.

It can be concluded that the ILS retrievals are very sensitive to various attenuators. The phase errors are more noisy than the ME amplitude. They indicate that the alignment of the interferometer was changed after either attenuator was inserted, and it caused more influence on optical modulation phase than optical modulation efficiency.

4.2 Potential strategy to adapt the incident intensity

As the ILS asymmetry is less critical than ILS width, the TCCON-prescribed maximal ME amplitude variation of 5 % within $\mathrm{OPD_{max}} = 45$ cm is taken as the upper limit (Wunch et al., 2015). As a result, the insertion of any of the attenuators no. 1–4 in front of or behind the interferometer could potentially be taken to adapt the incident intensity. Furthermore, we also verified some derivatives of attenuators no. 1–4 as shown in Fig. 9, which are also potential solutions. Selecting a smaller (bigger) entrance aperture to decrease (increase) incoming intensities is not optimal since the mechanical errors of different apertures may be non-negligible and inconsistent. This may be different from one instrument to the other; hence, the mechanical consistency of each field stop is recommended to be checked further before being used.

5 Summary

We investigated the sensitivity of ILS monitoring for ground-based high-resolution FTIR spectrometers with respect to various typical optical attenuators and positions. We confirmed that the ILS measurement using sun and internal lamp returned consistent results for the Bremen instrument. ILSs deduced from all scenarios of lamp cell measurements are compared. We observed that the ILS retrievals are very sensitive to various attenuators at different positions. The ILS disturbances with respect to the insertion of various attenuators in front of and behind the interferometer were quantified.

The insertion of any of the attenuators no. 1–4 or their derivatives in front of or behind the interferometer did not change the ILS much, and could potentially be taken to adapt the incident intensity. Selecting a smaller (bigger) entrance field stop (i.e., attenuator no. 5) to decrease (increase) incoming intensities is not optimal since the mechanical errors of different field stops may be non-negligible and inconsistent. This may be different from one instrument to the other; hence, the mechanical consistency of each field stop is recommended to be checked further before being used.

Data availability. The LINEFIT12 software is obtained on request from KIT Karlsruhe (http://www.imk-asf.kit.edu/english/897.php) (Hase et al., 1999). The used input files and the spectra are attached as a Supplement.

The Supplement related to this article is available online at doi:10.5194/amt-10-989-2017-supplement.

Competing interests. The authors declare that they have no conflict of interest.

Acknowledgements. This work is jointly supported by the Anhui Province Natural Science Foundation of China (grant no. 1608085MD79), the National Natural Science Foundation of China (grant no. 41530644, no. 41571130023, no. 41275038, no. 91544212, no. 41605018 and no. 41575021), the National Key Technology R&D Program of China (2014BAC22B00 and 2016YFC0200800), the National High Technology Research and Development Program of China (2014AA06A508, 2014AA06A511), the Scientific and Technological Project of Anhui Province (1301022083), the Special Project of Environmental Nonprofit Industry Research China (201409006), and the German Federal Ministry of Education and Research (BMBF) (grant no. 01LG1214A). All experiments are carried out at IUP, University of Bremen. The LINEFIT code is provided by Frank Hase, Karlsruhe Institute of Technology (KIT), Institute for Meteorology and Climate Research (IMK-ASF), Germany. The TCCON/NDACC networks are acknowledged for assistance and helpful discussions. We give great thanks to the anonymous referees for giving useful advice to improve this paper.

Edited by: J. Joiner
Reviewed by: three anonymous referees

References

Davis, S. P., Abrams, M. C., and Brault, J. W.: Fourier transform spectrometry, Academic Press, ISBN: 0-12-042510-6, 2001.

Duchatelet, P., Demoulin, P., Hase, F., Ruhnke, R., Feng, W., Chipperfield, M. P., Bernath, P. F., Boone, C. D., Walker, K. A., and Mahieu, E.: Hydrogen fluoride total and partial column time series above the Jungfraujoch from long term FTIR measurements: Impact of the line shape model, characterization of the error budget and seasonal cycle, and comparison with satellite and model data, J. Geophys. Res., 115, D22306, doi:10.1029/2010JD014677, 2010.

Feist, D. G., Arnold, S. G., Hase, F., and Ponge, D.: Rugged optical mirrors for Fourier transform spectrometers operated in harsh environments, Atmos. Meas. Tech., 9, 2381–2391, doi:10.5194/amt-9-2381-2016, 2016.

Hannigan, J. and Coffey, M.: semiautonomous FTS observation system for remote sensing of stratospheric and tropospheric gases, J. Atmos. Ocean. Tech., 26, doi:10.1175/2009JTECHA1230.1, 2009.

Hase, F.: Improved instrumental line shape monitoring for the ground-based, high-resolution FTIR spectrometers of the Network for the Detection of Atmospheric Composition Change, Atmos. Meas. Tech., 5, 603–610, doi:10.5194/amt-5-603-2012, 2012.

Hase, F., Blumenstock, T., and Paton-Walsh, C.: Analysis of the instrumental line shape of high-resolution Fourier transform IR spectrometers with gas cell measurements and new retrieval software, Appl. Optics, 38, 3417–3422, doi:10.1364/AO.38.003417, 1999 (data available at: http://www.imk-asf.kit.edu/english/897.php).

Hase, F., Demoulin, P., Sauval, A., Toon, G. C., Bernath, P., Goldman, A., Hannigan, J., and Rinsland, C.: An empirical line-by-line model for the infrared solar transmittance spectrum from 700 to 5000 cm^{-1}, J. Quant. Spectrosc. Ra., 102, 450–463, 2006.

Hase, F., Drouin, B. J., Roehl, C. M., Toon, G. C., Wennberg, P. O., Wunch, D., Blumenstock, T., Desmet, F., Feist, D. G., Heikkinen, P., De Mazière, M., Rettinger, M., Robinson, J., Schneider, M., Sherlock, V., Sussmann, R., Té, Y., Warneke, T., and Weinzierl, C.: Calibration of sealed HCl cells used for TCCON instrumental line shape monitoring, Atmos. Meas. Tech., 6, 3527–3537, doi:10.5194/amt-6-3527-2013, 2013.

Kohlhepp, R., Barthlott, S., Blumenstock, T., Hase, F., Kaiser, I., Raffalski, U., and Ruhnke, R.: Trends of HCl, $ClONO_2$, and HF column abundances from ground-based FTIR measurements in Kiruna (Sweden) in comparison with KASIMA model calculations, Atmos. Chem. Phys., 11, 4669–4677, doi:10.5194/acp-11-4669-2011, 2011.

Kurylo, M. J.: Network for the detection of stratospheric change (NDSC), SPIE Proceedings 1991, P. Soc. Photo-Opt. Ins., 1491, 168–174, 1991.

Messerschmidt, J., Macatangay, R., Notholt, J., Petri, C., Warneke, T., and Weinzierl, C.: Side by side measurements of CO_2 by ground-based Fourier transform spectrometry (FTS), Tellus B, 62, 749–758, doi:10.1111/j.1600-0889.2010.00491.x, 2010.

Miller, C. E., Crisp, D., DeCola, P. L., Olsen, S. C., Randerson, J. T., Michalak, A. M., Alkhaled, A., Rayner, P., Jacob, D. J., Suntharalingam, P., Jones, D. B. A., Denning, A. S., Nicholls, M. E., Doney, S. C., Pawson, S., Boesch, H., Connor, B. J., Fung, I. Y., O'Brien, D., Salawitch, R. J., Sander, S. P., Sen, B., Tans, P., Toon, G. C., Wennberg, P. O., Wofsy, S. C., Yung, Y. L., and Law, R. M.: Precision requirements for space-based X-CO_2 data, J. Geophys. Res., 112, D10314, doi:10.1029/2006JD007659, 2007.

Olsen, S. C. and Randerson, J. T.: Differences between surface and column atmospheric CO_2 and implications for carbon cycle research, J. Geophys. Res., 109, D02301, doi:10.1029/2003JD003968, 2004.

Schneider, M., Redondas, A., Hase, F., Guirado, C., Blumenstock, T., and Cuevas, E.: Comparison of ground-based Brewer and FTIR total column O_3 monitoring techniques, Atmos. Chem. Phys., 8, 5535–5550, doi:10.5194/acp-8-5535-2008, 2008.

Wang, Y., Deutscher, N. M., Palm, M., Warneke, T., Notholt, J., Baker, I., Berry, J., Suntharalingam, P., Jones, N., Mahieu, E., Lejeune, B., Hannigan, J., Conway, S., Mendonca, J., Strong, K., Campbell, J. E., Wolf, A., and Kremser, S.: Towards understanding the variability in biospheric CO_2 fluxes: using FTIR spectrometry and a chemical transport model to investigate the sources and sinks of carbonyl sulfide and its link to CO_2, Atmos. Chem. Phys., 16, 2123–2138, doi:10.5194/acp-16-2123-2016, 2016.

Washenfelder, R. A.: Column abundances of carbon dioxide and methane retrieved from ground-based near-infrared solar spectra, PhD thesis, California Institute of Technology, Pasadena, California, available at: http://resolver.caltech.edu/CaltechETD:etd-06022006-103523 (last access: 11 October 2015), 2006.

Wunch, D., Toon, G. C., Wennberg, P. O., Wofsy, S. C., Stephens, B. B., Fischer, M. L., Uchino, O., Abshire, J. B., Bernath, P., Biraud, S. C., Blavier, J.-F. L., Boone, C., Bowman, K. P., Browell, E. V., Campos, T., Connor, B. J., Daube, B. C., Deutscher, N. M., Diao, M., Elkins, J. W., Gerbig, C., Gottlieb, E., Griffith, D. W. T., Hurst, D. F., Jiménez, R., Keppel-Aleks, G., Kort, E. A., Macatangay, R., Machida, T., Matsueda, H., Moore, F., Morino, I., Park, S., Robinson, J., Roehl, C. M., Sawa, Y., Sherlock, V., Sweeney, C., Tanaka, T., and Zondlo, M. A.: Calibration of the Total Carbon Column Observing Network using aircraft profile data, Atmos. Meas. Tech., 3, 1351–1362, doi:10.5194/amt-3-1351-2010, 2010.

Wunch, D., Toon, G. C., Blavier, J.-F. L.,Washenfelder, R., Notholt, J., Connor, B. J., Griffith, D. W. T., Sherlock, V., and Wennberg, P. O.: The Total Carbon Column Observing Network, Phil. T. Roy. Soc. A, 369, 2087–2112, doi:10.1098/rsta.2010.0240, 2011.

Wunch, D., Toon, G. C., Sherlock, V., Deutscher, N. M., Liu, C., Feist, D. G., and Wennberg, P. O.: The Total Carbon Column Observing Network's GGG2014 Data Version, doi:10.14291/tccon.ggg2014.documentation.R0/1221662, 2015.